

Cancellation of reflections in planar antenna measuring systems via ESPRIT algorithm

Sara Burgos Martínez, M. Sierra Castañer, J.L. Besada Sanmartín

Signals, Systems and Radio communications Department

Polytechnic University of Madrid (UPM)

sburgos@teleline.es, m.sierra.castaner@gr.ssr.upm.es, besada@gr.ssr.upm.es

Abstract-

This paper presents an algorithm to cancel the reflections that appear in the anechoic antenna measurement systems due to low frequency bands, AUT and probe supports... The algorithm is based on a modification of the ESPRIT [1-3] direction of arrival method and needs a very low number of frequencies to work – that is, a strict requirement in antenna measurement system. Actually, this algorithm will be applied to a planar near field scanner.

INTRODUCTION

One of the most important drawbacks of the antenna measuring systems in anechoic chambers is the difficulty to cancel all the reflections. When a high precision in measurements is required, the fact that certain reflection rays are involved may affect the radiation diagram and may cause errors over the specified limits.

The reflection cancellation algorithms that exist are based on multifrequency measurements and they are generally impracticable, due to the time of measuring they need. There are some procedures based on FFT or Matrix Pencil Method to reduce the effect of reflections [4-7] but they need a very large number of measurements at different frequencies.

In this paper, an algorithm that requires a reduced number of frequencies, of interference cancellations is explained. It's based on modifications of Estimation of Signal Parameters Via Rotational Invariance Techniques (ESPRIT) and its application in planar antenna measuring systems.

This presentation is organized as follows. In the next section, the planar measuring system of the ETSIT Polytechnic University of Madrid, where the measurements are to be fulfilled, is presented. The algorithm described to obtain the detected angles is elucidated in Section II. In section III, the signal reconstruction process is described. Then, in Section IV, the simulations and the results are presented. Finally, the conclusions obtained through the analysis of the results are discussed.

I. PLANAR MEASURING SYSTEM OF THE ETSIT-UPM

The UPM has an antenna measurements laboratory with three anechoic chambers: one near field spherical system, one arc system and one big chamber (15.2 x 7.9 x 7.3 meters) shared by two systems: one compact range and one spherical, cylindrical and planar near field system.

This last system occupies an area of 6 x 7.9 x 7.3 meters. The planar scanner has a useful surface of 4.75 x 4.5 meters, with errors in normal dimension lower than 240 μm (peak to peak) that allow a maximum frequency of 40 GHz. The system also has a linear slide (to place the AUT), a roll positioner (for polarization horn) and a roll over azimuth positioner (for the spherical and cylindrical system).

This system is equipped with rotary joints, microwave cables and an antenna network analyzer to measure until 40 GHz. The anechoic material allows the measurements from 900 MHz, and the maximum diameter of the Antenna Under Test is 2.5 meters.

Finally, the system is completed with a position controller and the required software to convert the acquired near field in far field values. Figure 1 shows a photograph of the planar scanner.

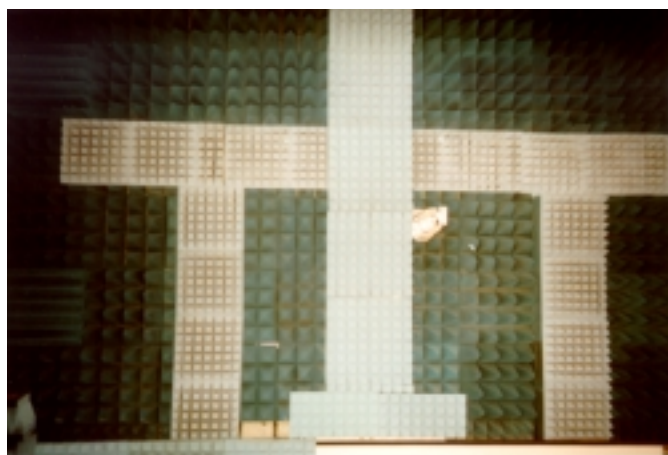


Fig 1: Planar scanner at UPM.

II. METHOD DESCRIPTION

This technique is based on the implementation of the high-resolution direction-of-arrival (DOA) method, called ESPRIT. To simplify the detection algorithm, the number of signals has been set. To attain a higher precision of the detection angle, this technique has been repeated N times, where N represent the number of frequencies, which are randomly generated around the central frequency (f_0).

A. SIGNAL GENERATION

The objective of this algorithm is to determinate the direction-of-arrival (DOA) of “L” planar wave fronts, which have its focal point separated from a higher “h” from the receiver array.

To allow this, first of all, the signal generation has to be completed. In order to describe mathematically the effect of the translation invariance of the array, it is useful to express the receiver array as being separated in two subarrays, identical in every aspect although physically distance from each other by a known displacement “d”.

Namely, two subarrays must be considered, each one formed with one element less than the general array and separated by a quantity which coincides with the displacement between elements.

Furthermore, each one of the wave fronts evaluated are assumed to be narrow-band sources, centred at same frequency evaluated (f_i). As far as the arrival directions are concerned, they are going to be estimated in the p direction only, so as to simplify the problem. Besides, those wave fronts are supposed to come from a transmitter array, shaped by M elements. Accordingly, each signal arrives from M positions and strikes with a variable angle (φ) depending on the transmitter position. For that reason, the angle of incidence will have “L” components according to the number of wave fronts taken into account.

In this paper, only two wave fronts have been studied. The first one corresponds to the direct ray and the second one is the one produced by the reflection. When the direct signal is considered, the angle “ φ ” depends only on the height of the focal point (h) and on the positions evaluated in transmission as well as in reception – with regard to a reference, which is the central element of the array. However, the angle “ φ ” analysed for the reflection requires additionally the distance existing between the reference and the position of the element that causes the reflection (D).

Each one of the emitted signals is multiplied by the matrix “A” – steering matrix – for each element of the two subarrays. This matrix contains the information about the distance between the elements of the transmitter and the receiver measured, which depends on the height “h” and on the angle φ , as it is shown below:

$$r_p > \frac{h}{\cos \kappa_p}, p > 1, \dots, L \quad (1)$$

where:

- L is the number of signals evaluated
- $\varphi = [\varphi_1, \dots, \varphi_L]$. Note that φ_p is the direction-of-arrival of the p th signal.

For each of the signal contemplated, the steering matrices of each subarray formed by n elements are:

÷ Analysing the first subarray:

$$A_x(t) > e^{jk r_1}, r_1 > r_2, \dots, r_n, \downarrow k > 2 - \theta - f/c \quad (2)$$

÷ Taking into consideration the second subarray:

$$A_y(t) > e^{jk r_2}, r_1 > r_2, \dots, r_n, \downarrow k > 2 - \theta - f/c \quad (3)$$

Therefore, the steering matrix expresses the effect that the field experiences in the receiver array and can be written as follows:

$$A > A_x; A_y \downarrow \quad (4)$$

Besides, the signals required are supposed to be correlated. That is the reason why they are modelled as having a fixed level, which could be different for the direct and the reflected signal. This is not the case in this presentation, where the magnitude mentioned is assumed to be the same for both of them.

To obtain the signals arriving in each of the “2n” elements of the receiver array, the steering matrix is multiplied by the signals coming from each of the “M” elements of the transmitter.

And then, to get the total signal received, the “M” signals captured in each of the elements of the receiver array are added.

As it is supposed to be a real system, additive noise is present in all the elements of the arrays. Thus, noise estimated is assumed to be a stationary zero-mean random process and is also included.

Taking a vector notation for the outputs of the “M” elements of the transmitter array, and considering the Gaussian noise, the measurement model of the signal processing problem is given by:

$$x_i(t) > \sum_{k=1}^M s_k(t) A_k(f, \rho_p)^*, n_{x_i}(t), \quad (5)$$

$$i > 1, \dots, 2n \downarrow p > 1, \dots, L \downarrow$$

where the arrival directions are each of the θ directions.

B. ARRIVAL ANGLE DETECTING METHOD ESPRIT

The ESPRIT method (Estimation of Signals Parameters Via Rotational Invariance Techniques) is based on the assumption that the noise employed is uncorrelated with the signals.

Using the relation between induced subspaces by the two subarrays, which depends on the arrival angle, the DOA (direction-of-arrival) can be obtained.

In other to calculate the arrival angle, the TLS (Total Least Squares) ESPRIT algorithm based on a covariance approach can be employed as it is summarised in the following steps:

1. An estimation of the autocorrelation matrix from the measurements is found. For this reason, the autocorrelation is approximate using N samples of the signals as it is shown below:

$$\hat{R}_{zz} > \frac{1}{N} X^* X^H \quad (6)$$

where N indicates the number of frequencies evaluated.

2. A generalized eigendecomposition of the previous matrix is computed in its eigenvectors and eigenvalues.
3. Then the number of sources is estimated. In this presentation, this integer has been fixed.
4. The previous eigenvectors is decomposed into eigenvectors of the “x” subarray and of the “y” subarray. The first n components of each vector are considered to belong to the subarray “x” and the next “n” eigenvectors to the subarray “y”. The number of vectors of each subspace will be the quantity of signals considered in the step next.
5. The eigendecomposition TLS (*Total Least-Squares*) is determined by using the following method:

$$\begin{aligned}
 E &> [E_x E_y]^H - [E_x E_y] \\
 E &> \begin{bmatrix} E_{11} & E_{12} \\ E_{21} & E_{22} \end{bmatrix} \\
 \zeta &> -E_{12} - E_{22}^{-1}
 \end{aligned} \quad (7)$$

6. The eigenvalues of the matrix ζ are calculated: $\gamma_1 \dots \gamma_L$
7. Finally, the arrival angles (DOA) are analyzed as follows:

$$\hat{\rho}_k > a \sin \left(\frac{c - \arg \gamma_k}{d - \xi_0} \right) \quad (8)$$

III. SIGNAL RECONSTRUCTION

Once the arrival angles have been obtained, the reconstruction process could begin. This procedure is repeated for each of the considered frequencies and can be described as follows:

1. First of all, an estimation of the steering vector for the direct signal considering each element of the receiver array is achieved. It must be taken into account that, for the covered distance calculation, the position of the transmission array and the height between the transmitter and the receiver are employed.
2. After that, an evaluation of the steering vector for the reflection is completed by obtaining each element of the receiver array. To enable this, the field studied is considered to be a far field, which depends of the arrival angle detected for the studied reflection (θ_{ref}). In this case, the parameters used in the traversed interval are the position of the transmission array and the sinus of angle θ_{ref} .
3. Then, the steering matrix is defined by:

$$\mathbf{A}_{\text{estim}} > [\mathbf{A}_{\text{estim,direct}}, \mathbf{A}_{\text{estim,reflected}}] \quad (9)$$

4. The next phase involves solving the equation system used to reconstruct the signals ($s(t) = [s_1(t), \dots, s_{2n}(t)]$). In this system formed by N equations – where N is the number of frequencies – the parameters involved are the estimated steering matrix ($\mathbf{A}_{\text{estim}}$) and the total signals ($x(t) = [x_1(t), \dots, x_{2n}(t)]$) stated in the relation (5). Note that those signals are independent from the frequency taken into account.
5. To finish, the reconstructed signals are multiplied by the estimated steering matrix, and can be expressed as:

$$\hat{x}_i(t) > \mathbf{A}_i(f, \rho > 0) \cdot s_i(t) \quad (10)$$

In fact, the comparison between signals can not be fulfilled unless this calculation is achieved. Namely, it is necessary to multiply $s(t)$ by $\mathbf{A}_{\text{estim}}$ in order to compare $s(t)$ with the signals computed in the generation signal model, as described in the previous section.

With those results, it is possible to reproduce the amplitude and phase of all the signals generated, that is to say:

- ÷ the total signal – representing the sum of direct and reflected signals to which Gaussian noise is added,
- ÷ the ideal signal – including only the noisy directed signal,
- ÷ the reconstructed signal.

That enables to compare all the signals and to calculate the medium quadratic error between them.

IV. PERFORMED SIMULATIONS AND RESULTS

In this section, simulation and results are presented to illustrate the performance of the designed algorithm.

Many simulations have been performed, exploring different aspects by changing the parameters involved. In fact, in order to observe the evolution of the precision obtained, certain factors have been increased while setting the others. The analysed variables have been: the number of frequencies (N), the number of elements in the transition array (M) and in the receiver subarray (n), both separated half wavelength at central frequency.

For each, the amplitude and phase diagrams have been presented. Besides, the detected arrival angles (Θ_d and Θ_{ref}), the error created because of their estimation and the errors in the reconstruction and reflection process ($E_{\text{reconstruct}}$ and $E_{\text{reflection}}$ respectively) have also calculated.

From all these studied scenarios, only two of the most relevant are exposed, which are:

- ÷ **Case 1:** When $M=3$, $n=14$ and **N** increases.
- ÷ **Case 2:** When $N=3$, $n=14$ and **M** increases.

In those situations, the height between transmitter and receiver is set to one meter and the reflection element is supposed to be 2.85 meters from the reference. As the number of sources is assumed to be known in the implementation of ESPRIT, here it has been fixed to two. Furthermore, the group of frequencies randomly generated have been located around the central frequency $f_0=10$ GHz. Finally, it must be taken into account that both signals – direct and reflected – have the same power (30 dB over the noise level).

1. Case1: M=3, n=14 and N increases

When $M=3$ and $n=14$, the next table shows the results achieved in these simulations:

Parameter	N = 3	N = 5	N = 8	N = 15	N = 35
Θ_d (°)	0.0513	0.0903	0.0695	0.0773	-0.0438
Θ_{ref} (°)	-78.0043	-79.9578	-81.5339	-79.6274	-80.5411
E_{Θ_d} (°)	0.0513	0.0903	0.0695	0.0773	0.0438
$E_{\Theta_{\text{ref}}}$ (°)	2.0451	0.0916	1.4846	0.4220	0.4917
$E_{\text{reconstruct}}$	0.0176	0.0068	0.0010	7.7498e-4	5.386e-4
$E_{\text{reflection}}$	0.1007	0.1029	0.1007	0.1021	0.1010

Table 1: Results increasing N, $M=3$, $n=14$

In particular, when $N=15$, the amplitude and the phase have the following diagrams:

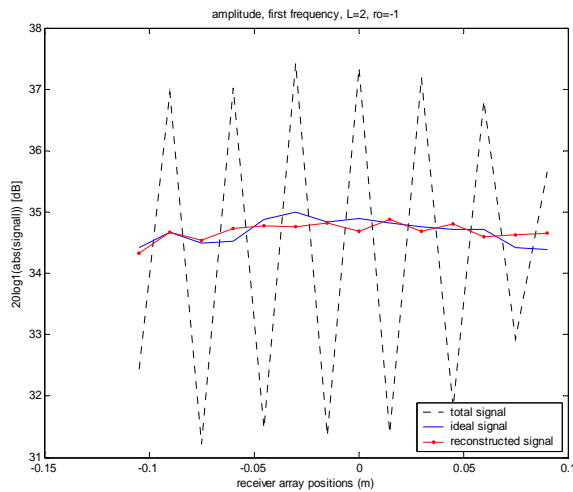


Fig 2: Amplitude when $M=3$, $n=14$, $N=15$

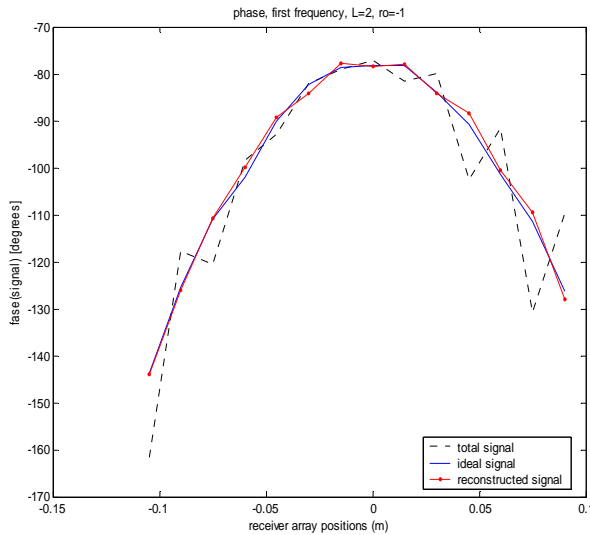


Fig 3: Phase when $M=3$, $n=14$, $N=15$

2. Case2: $N=8$, $n=160$ and M increases

When $N=8$ and $n=160$, the next table illustrates the results reached in this case:

Parameter	$M = 5$	$M = 13$	$M = 23$	$M = 43$	$M = 63$
Θ_d (°)	0.6101	0.3993	0.7503	0.3837	0.2508
Θ_{ref} (°)	88.2519	88.1127	88.4898	-88.1858	-89.2531
E_{Θ_d} (°)	0.6101	0.3993	0.7503	0.3837	0.2508
$E_{\Theta_{ref}}$ (°)	8.2026	8.0633	8.4404	8.1365	9.2037
$E_{reconstruct}$	0.0260	0.0118	0.0094	0.0084	0.0080
$E_{reflection}$	0.1806	0.0714	0.0430	0.0024	0.0054

Table 2: Results increasing M , $N=8$, $n=160$

Particularly, when $N=23$, the amplitude and the phase have the following diagrams:

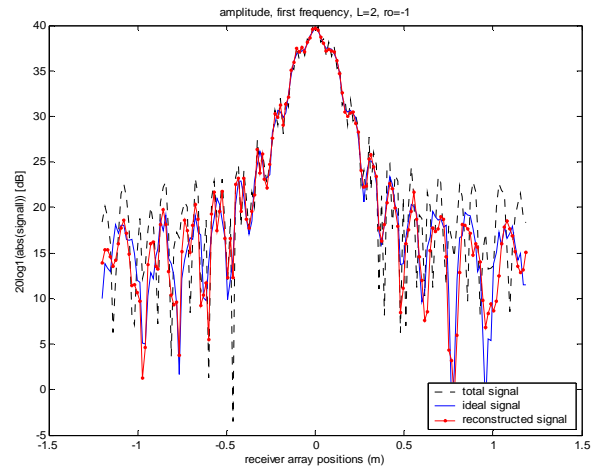


Fig 4: Amplitude when $N=8$, $n=160$, $M=23$

These results indicate that the precision in the reconstruction algorithm increases as more frequencies are used – N rises. In fact, when 8 frequencies are employed, accurate results are achieved. Note also that the errors obtained in those signals ($E_{reconstruction}$) have been reduced quite a lot comparing then to those found for the total signals.

Case 2 shows that reconstruction errors decrease as M rises, although the reconstruction is still very good for small dimensions of AUT. However, for large antennas the error due to reflections is quite low. In this case, the algorithm cannot obtain better results.

V. CONCLUSIONS

This paper presents an algorithm to cancel the reflections in near field systems, using an estimation of the angles of arrival signals based upon ESPRIT method. The simulations show good estimations of the signals. However, this can be complemented by checking these results with antenna measurements and extending to a planar system, instead of using a linear system.

REFERENCES

- [1] R. Roy and T. Kailath, "ESPRIT – Estimation of signal parameters via rotational invariance techniques", IEEE Trans. Acoust., Speech, Signal Processing, Vol. 37, No. 7, pp. 984-995, July 1989.
- [2] M. Wax and T. Kailath, "Detection of Signals by Information Theoretic Criteria", IEEE Trans. Acoust., Speech, Signal Processing, Vol. ASSP-33, No. 2, pp. 387-392, April 1985.
- [3] R. Roy, B. Ottersten, L. Swindlehurst, and T. Kailath, "Multiple invariance ESPRIT", IEEE Trans. Acoust., Speech, Signal Processing, Vol. 40, No. 4, pp. 867-881, April 1992.
- [4] T. K. Sarkar and O. Pereira "Using the Matrix Pencil Method to Estimate the Parameters of a Sum of Complex Exponentials" IEEE, Antennas and Propagation Magazine, Vol. 37, No. 1, pp. 44-54, February 1995.
- [5] R. S. Adve, T. K. Sarkar, O. M. C. Pereira-Filho and S. M. Rao, "Extrapolation of Time-Domain Responses from Three-Dimensional Conducting Objects Utilizing the Matrix Pencil Method", IEEE Transactions on Antennas and Propagation", Vol. 45, No. 1, pp. 147-156, January 1997
- [6] Y. Hua and T. K. Sarkar, "Generalized pencil-of-function method for extracting poles of an EM system from its transient", IEEE Transactions on Antennas and Propagation", Vol. 37, No. 2, pp. 229-234, January 1989
- [7] S. Loredó Rodríguez, M. Rodríguez Pine, F. Las Heras Andrés, T. K. Sarkar, "Cancelación de ecos en cámaras de medida no anecoicas", Simposio Nacional U.R.S.I. A Coruña, Septiembre 2003.